The Influence of the Starting Cu–Sn Phase on the Superconducting Properties of Subsequently Reacted Internal-Sn Nb_3Sn Conductors

Michael T. Naus, Peter J. Lee, and David C. Larbalestier

Abstract—**We have studied the reaction conditions and properties of a high-Sn, internal-Sn Nb_3Sn conductor whose overall Cu–Sn composition was Cu–29at.%Sn. By adjusting the mixing heat treatment during which the Cu and Sn interdiffuse prior to A15 reaction, it is possible to substantially surround the Nb filaments with α and/or ε-phase Cu–Sn. It does not seem possible, however, to homogeneously mix the Cu and Sn prior to A15 formation. The T_c distributions, measured both by SQUID and heat capacity, showed no dependence on significantly different mixing heat treatments. Magnetization measurements at 4.2 K and 12 K also showed that there were no significant differences in the H^*, H_{c2} and J_c (as indicated by Δm). This implies that the composition and reaction behavior of the A15 phase is independent of the Cu–Sn phase in contact with the Nb filament prior to the reaction heat treatment and that scoping experiments on high-Sn, high-J_c internal-Sn conductors can be considerably simplified. Our studies suggest a new Cu–Nb–Sn intermetallic phase with a composition of Cu–23at.%Nb–62at.%Sn.**

Index Terms—**Copper-Tin Mixing, Internal Tin, Niobium-Tin, Heat Treatments.**

I. Introduction

THE optimization of heat treatments (HT) for internal-Sn Nb_3Sn superconducting wire has often been debated because multiple HT variants are possible. Each HT variant must perform two functions: (1) mix the Cu and Sn, and (2) form the A15 phase. The mixing portion of the HT usually takes the form of several strategically placed hold temperatures, but can be a slow temperature ramp [1]. Most hold temperatures are chosen to avoid liquefaction of Sn and the Cu–Sn intermetallic η-phase, as their melting points (232°C and 415°C, respectively) are below typical Nb_3Sn reaction temperatures (> 600°C). The hold temperatures are designed to allow these phases to transform into a higher melting point, more Cu-rich phase via solid state diffusion prior to any increase in HT temperature.

Although uniform Sn distribution is in principle the goal of the mixing HT, it seldom happens in practice. While mixing studies are always particular to each composite design, it has been seen that complete phase transformation into a higher melting point phase does not always occur. [2] and [3] reported that pure Sn remained in the core after the manufacturers' suggested 200°C Sn-removal HT step, which calls into question the true value of this step. Also, it has been reported [3], [4] that the Cu–Sn matrix is not single phase just prior to reaching the Nb_3Sn reaction temperature. Homogenization experiments on ITER conductors have shown that it is not possible to fully mix the Cu and Sn in a reasonable time [5]. Since 1/3 to 1/2 of the total HT time is spent on *incomplete* Cu–Sn mixing, the importance of achieving full homogenization is often questioned.

Cu–Sn inhomogeneity potentially sets up a situation where different Nb filaments are in contact with different Cu–Sn phases. Based upon the Cu–Nb–Sn phase diagram [6], one might expect that this would affect the A15 composition of individual filaments and thus their superconducting properties. Here we have investigated the Cu–Sn phases formed in a high-Sn, high critical current density (J_c) wire using various Cu–Sn mixing heat treatments. We then gave some of these samples a subsequent A15 reaction HT to examine the superconducting consequences of the different local Cu–Sn environments present at the time of reaction.

II. Experimental Procedure

The conductor (designated CRe1912) (Fig. 1) was a high-Sn, high-J_c conductor manufactured by the Modified Jelly-Roll, internal-Sn process at Teledyne Wah Chang (now Wah Chang). The 0.5 mm diameter wire contained 54 bundles, each with a Sn–2wt.%Mg alloy core surrounded by a double wrap of Cu and expanded Nb–1wt.%Ti mesh all surrounded by a Nb diffusion barrier. The overall Cu–Sn composition within the diffusion barrier was Cu–29at.%Sn, which is slightly higher in Sn than the Cu–Sn phase ε (Cu–25at.%Sn). At 0.6 mm diameter, the transport J_c(4.2 K, 12 T) attained 2195 A/mm^2 [7]. The manufacturer's recommended HT for this composite is 120h/185°C + 72h/340°C + 180h/650°C. This was used as a guide for our heat treatments.

A. Cu–Sn Phase Formation

The ends of ~80 mm long samples were electroplated with Cu to prevent Sn leakage. The samples were then sealed in evacuated quartz tubes under ~30 mTorr Ar and inserted into a pre-heated furnace for 24 and 150 hours. The temperatures used were approximately 10°C above and below the < 600°C temperature invariants of the Cu–Sn system (see Table I for temperatures used). The quartz tubes were water quenched upon removal from the furnace. Approximately 10 mm was

Manuscript received September 17, 2000.

This work was supported by the U.S. Department of Energy – Office of Fusion Energy Sciences (DE-FG02-86ER52131) and Division of High Energy Physics (DE-FG02-91ER40643), and benefited from NSF-MRSEC (DMR-9632427) supported facilities.

Authors are with the Applied Superconductivity Center, University of Wisconsin, Madison WI 53706 USA (telephone: 608-263-4462, e-mail: naus@cae.wisc.edu).

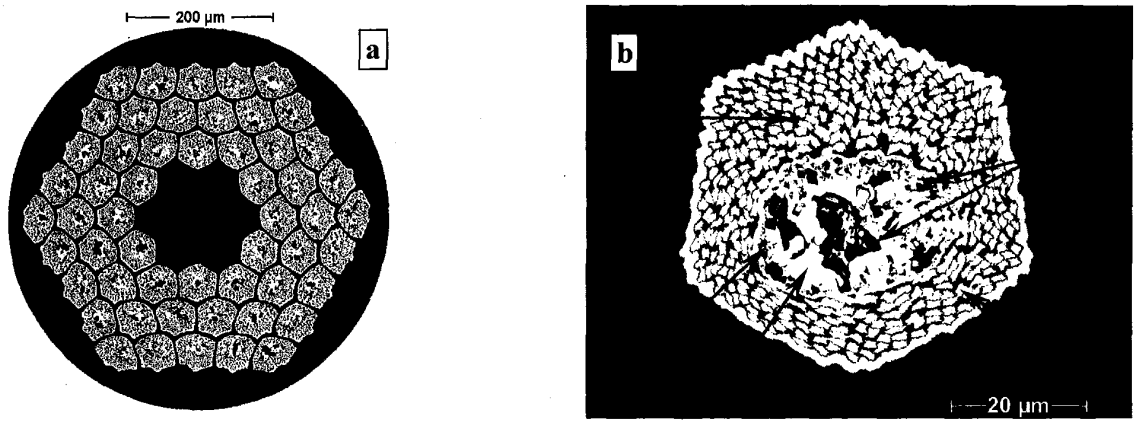

Fig. 1. SEM-BE images of the wire (a) and bundle (b) cross-sections prior to heat treatment. Mg-Cu-Sn ternary particles were seen in the core prior to any heat treatment. The voids are most likely a polishing artifact.

removed to avoid end effects. The Cu–Sn phases were determined by energy dispersive spectroscopy (EDS), backscatter scanning electron microscopy (SEM-BE) and light microscopy.

B. A15 Phase Formation

The samples heat treated for 150 hours at 362°, 402°, 428°, 510° and 533°C were then reacted to form the A15 phase. The remaining ~55 mm length from the Cu–Sn investigation was re-plated with Cu, sealed in quartz tubes as before, inserted into pre-heated furnaces at 650°C for 180 hours and water quenched upon removal. The critical temperatures (T_c) were measured inductively using a Superconducting Quantum Interference Device (SQUID) by zero field cooling the sample to 6 K and then measuring upon warming in an applied field of 5 mT. T_c was also evaluated by heat capacity (C_p) measurements to alleviate concerns about shielding of the filament interior in the inductive measurements. The irreversibility field (H^*) and upper critical field (H_{c2}) were measured using a Vibrating Sample Magnetometer (VSM) in a 14 T magnet swept at 0.6 T/min. The magnetic field direction was perpendicular to the wire axis. H_{c2} was determined as the field at which the magnetic moment deviated from the paramagnetic background moment. H^* was defined at both the field of hysteretic magnetization loop closure ($H^*_{\text{Loop Closure}}$) and at the extrapolation of the Kramer plot [8] to zero (H^*_{Kramer}). The width of the hysteretic magnetization loop, Δm, is proportional to J_c and thus the Kramer plots were generated by plotting $\Delta m^{1/2} B^{1/4}$ versus B. In order to examine the relative J_c values, Δm was normalized to sample mass.

TABLE I
Cu-Sn PHASES DETECTED AFTER THE MIXING HEAT TREATMENTS

Heat Treatment Temperature (24h/150h)	Cu-Sn Phases α	β	γ	δ	ζ	ε	η	Pure Sn	Mg-Cu-Sn Ternary
218°/217°C	✓✦					✓✦	✓✦	✓	✓✦
237°/239°C	✓✦					✓✦	✓✦		✓✦
335°/342°C	✓✦					✓✦	✓✦		✓✦
360°/362°C	✓✦					✓✦	✓✦		✓✦
401°/402°C	✓✦					✓✦	✓		✓✦
426°/428°C	✓✦					✓✦			✓✦
510°/510°C				✓✦		✓✦			✓✦
528°/533°C				✓✦		✓✦			✓✦
569°/569°C	✦		✓	✓		✓			✓✦
599°/604°C	✓✦ ✣		✣		✣				✓✦

✓ = 24 hour heat treatment; ✦ = 150 hour heat treatment; ✣ = Refined microstructure seen after the 24h heat treatment might have been formed from a eutectoid decomposition of this phase.

III. RESULTS

A. Observed Cu–Sn Phases

The Cu–Sn phases found after the mixing heat treatments are compiled in Table I, where they are arranged from lowest to highest Sn content. At low temperatures, diffusion is clearly incomplete and multiple phases formed, but as temperature and time increased, the trend was toward ε-phase, which is close to the overall Cu–Sn composition. It is interesting to note the absence of visible δ-phase between α and ε phases above 350°C where it is thermodynamically stable. Mg was found only in Cu–Sn–Mg ternary compounds.

We have found a Cu–Nb–Sn structure growing into the core region after the mixing HT (Fig. 2). SEM-BE images showed this to be single phase at HT temperatures ≤ 402°C and multi-phase at ≥ 426°C. Using EDS analysis, the compo-

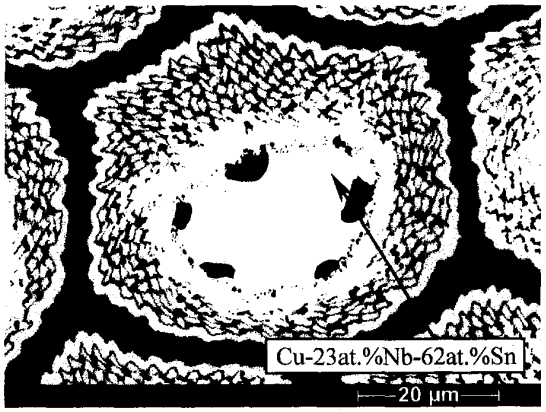

Fig. 2. SEM-BE image of a Cu-Nb-Sn ternary phase growing into the core region after a heat treatment of 150h/362°C. A similar structure surrounds the inner rows of filaments.

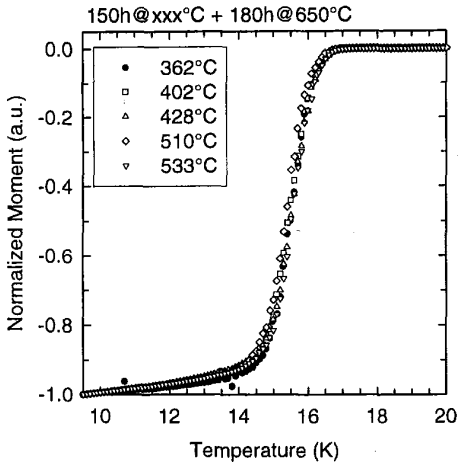

Fig. 3. Inductively measured T_c traces after 5 different mixing heat treatments. The mixing heat treatment had no effect on T_c. The data has been normalized to account for differences in wire volume.

sition of the single phase structure was determined to be Cu–23at.%Nb–62at.%Sn and that of the multi-phase structure Cu–20at.%Nb–30at.%Sn. Similar structures were present amongst the inner rows of filaments after all mixing heat treatments, but their size was too small for accurate EDS examination. Upon re-examination of the wires studied in [5], similar fine structures were seen around individual Nb filaments, but only when a Cu–Sn intermetallic was in contact with the Nb. These structures were also too small to be analyzed by EDS.

B. Superconducting Properties

Inductive T_c measurements of wires homogenized for 150 hours at 362°, 402°, 428°, 510° and 533°C followed by an A15 reaction HT of 180 hours at 650°C are shown in Fig. 3. There was no discernible dependence in the T_c traces on different mixing HT temperatures. The transition mid-point for all curves was ~15.5 K. Consistent with the SQUID data, C_p measurements on the samples with mixing HT temperatures of 362°, 428° and 533°C (Fig. 4) also showed no significant difference in the T_c distribution, though the values were higher (see discussion). Due to the large phonon background in the C_p measurements, the superconducting contribution was partially masked. However, the phonon contribution follows a cubic relation and is easily removed. The minor differences at lower temperature, where the superconducting signal is small, are not deemed significant.

Table II shows H_{c2}, $H^*_{\text{Loop Closure}}$ and H^*_{Kramer} at 4.2 K and 12 K for mixing heat treatments at 362°, 428° and 533°C. All differences (< 3%) are near the measurement uncertainty, but there may perhaps be a small but statistically significant decrease in H^* as mixing HT temperature increases. The differences in the magnetization loop widths, Δm, were also very small (< 3%).

IV. Discussion

Based upon the data in Table I, it is unlikely that the Sn can be uniformly distributed prior to the beginning of the A15 reaction step in high-Sn, internal-Sn composites with subbundles ~50 μm in diameter. This inhomogeneity in the Cu–Sn matrix does not, however, have a significant influence on the T_c distribution, H^*, H_{c2} or J_c (as indicated by Δm) of the subsequently formed A15 phase in fully reacted wires. Therefore, the potentially enormously variable parameter space of the mixing HT is apparently largely removed. This result, if confirmed for other high-Sn wires, could greatly simplify evaluation of the influence of heat treatments on superconducting properties.

The apparent independence of the superconducting properties on the Cu–Sn mixing HT indicates that significant HT shortening is possible, at least for short sample experiments. However, there is anecdotal evidence that wire burst can occur without adequate Cu-Sn mixing in long lengths of wire. The common explanation is that excessive hydrostatic pressure due to Sn liquefaction causes weak regions of the diffu-

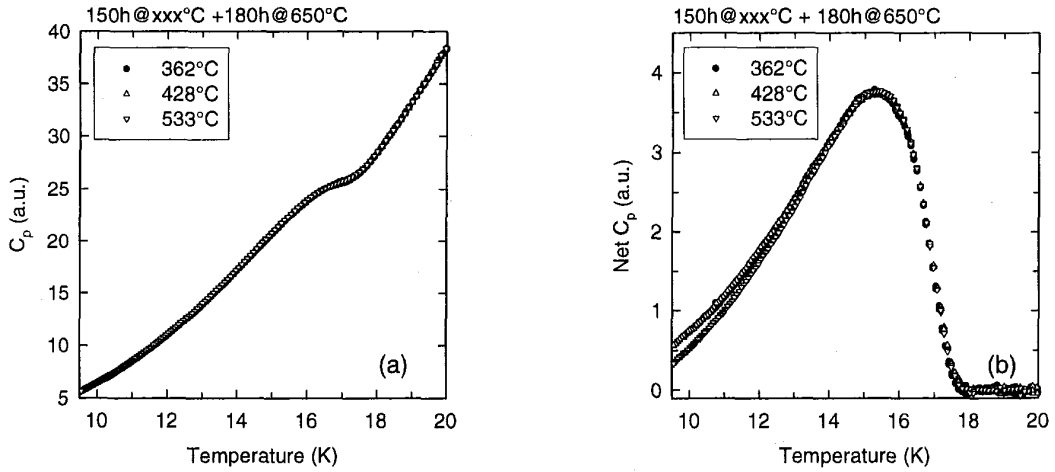

Fig. 4. Heat capacity of the entire sample (a) and the superconducting contribution (b) after 3 different mixing HT temperatures. There is no significant difference in the T_c distribution due to different mixing heat treatments. The large background phonon signal seen in (a) partially masks the superconducting contribution, but it follows a cubic relation and is easily subtracted to show the superconducting contribution only. The data in both curves has been adjusted by a scaling factor to facilitate comparison.

TABLE II
H^*, H_{c2} AND NORMALIZED HYSTERESIS LOOP WIDTH COMPARISONS

		150h/362°C +	150h/428°C + 180h/650°C	150h/533°C + 180h/650°C	% Deviation
Δm/mass (emu/mg)	4.2 K, 12 T	3.82×10^{-3}	3.75×10^{-3}	3.84×10^{-3}	2.4
	12 K, 5 T	1.39×10^{-3}	1.37×10^{-3}	1.35×10^{-3}	2.9
H^*_{Kramer} (T)	4.2 K	24.0	23.5	23.3	3.0
	12 K	9.3	9.1	9.0	2.2
$H^*_{Loop\ Closure}$ (T)	12 K	11.4	11.4	11.4	0.0
H_{c2} (T)	12 K	13.2	13.1	13.2	0.8

sion barrier to burst. Therefore, shortening of the mixing HT may prove detrimental in long lengths because of the greater statistical probability of having a weak region in the diffusion barrier.

Liquid formation may also encourage filament motion, as may the movement of the ε-α Cu–Sn phase boundary through the bundle [9], both tending to increase hysteretic loss. However, filament motion is not a concern for the high-Sn conductors of this study because the filaments are so close that they come into contact after the A15 reaction, regardless of the mixing HT used.

An issue to address in our superconducting evaluations is the averaging over the inhomogeneous A15 reaction layer. H_{c2} and $H^*_{Loop\ Closure}$ from VSM data represent the highest field transitions in the sample, presumably those due to the most stoichiometric and least strained regions, since lower transitions are masked by higher ones. However, H^*_{Kramer} is derived from an extrapolation that is weighted to lower field data and better approximates average properties. Kramer extrapolations are generally reported as H_{c2}; however previous work with Nb–Ti F_p plots indicates that such extrapolations are more representative of H^* [10].

The T_c measurements show inhomogeneity within each filament bundle. The inductive T_c transitions occurred between 14.5 and 16 K (10-90%) and between ~15 and 18 K in the C_p measurements. Long-range shielding currents dominate the inductive measurements, whereas the C_p measurements give a true volumetric T_c weighting. The difference implies that the best A15 regions observed by the C_p measurements (T_c > 16 K) are on a much smaller scale than the whole filament bundle. Both data sets show that much of the A15 exhibits significant T_c depression below the unstrained stoichiometric value of >18 K.

We can find no hitherto reported Cu–Nb–Sn intermetallic phases. However, to the limits of our SEM-BE image resolution (< 50 nm), a single phase Cu–23at.%Nb–62at.%Sn ternary formed below ~402°C. Due to their small areas, it is unknown whether any of the individual phases within the multi-phase Cu–Nb–Sn material, which formed above 426°C, are already known binary phases or Cu–Nb–Sn ternaries. It is unknown what role, if any, the Cu–Nb–Sn phase plays in A15 formation.

There is an often expressed concern in the Nb_3Sn community that δ-phase has a deleterious effect in A15 formation, although supporting evidence is lacking. We expected that δ-phase would form above 350°C between the α and ε phases. However, no sign of δ-phase at 360°, 401° and 427°C was seen. [11] and [12] also noted that δ-phase did not always form in Sn-plated Cu sheet at temperatures between ~350°C and ~400°C. We conclude that δ-phase formation has garnered more attention than is warranted.

V. CONCLUSIONS

We have tabulated the Cu–Sn phases found in a high-Sn, high-J_c, internal-Sn composite after 24 and 150 hour at 10 different temperatures. It appears that complete mixing of the Cu and Sn is not possible. The Nb filaments are then forced to react with different Cu–Sn phases depending upon their position within the bundle. However, there do not appear to be any significant consequences for the superconducting properties in fully reacted samples, suggesting that it does not matter how one homogenizes the Cu and Sn. This opens the door to significantly decreasing mixing HT time, at least in short sample scoping experiments. We have also observed a Cu–Nb–Sn intermetallic phase which has a composition of Cu–23at.%Nb–62at.%Sn.

REFERENCES

[1] M. Takayasu, R. A. Childs, R.N. Randall, R. J. Jayakumar and J. V. Minervini, "ITER niobium-tin strands reacted under model coil heat-treatment conditions," *IEEE Trans. Appl. Supercond.*, vol. 9 (2), pp. 644-647, 1999.

[2] R. Taillard and C. Verwaerde, "Phase transformations during the manufacturing process of Nb_3Sn superconducting composites," Proc. Euromat95, Venice, pp. 471-474, 1995.

[3] D. R. Dietderich, J. Glazer, C. Lea, W. V. Hassenzahl and J. W. Morris, Jr., "The critical current density and the microstructural state of an internal tin multifilamentary superconducting wire," *IEEE Trans. Magn.*, vol. 21 (2), pp. 297-300, 1985.

[4] B. A. Glowacki, "Influence of the tin diffusion process in multifilamentary Nb-Cu-Sn-Mg-Ta wire on Nb_3Sn interfilamentary bridging," *IEEE Trans. Appl. Supercond.*, vol. 7 (2), pp. 1520-1523, 1997.

[5] M. T. Naus, P. J. Lee and D. C. Larbalestier, "The interdiffusion of Cu and Sn in internal Sn Nb_3Sn superconductors," *IEEE Trans. Appl. Supercond.*, vol. 10 (1), pp. 983-987, 2000.

[6] P. Villars, A. Prince and H. Okamato, *Handbook of Ternary Alloy Phase Diagrams*, ASM International, vol. 8, 1995, pp. 9753-9757.

[7] P. D. Jablonski and J. C. McKinnell, "An improved method for making high field critical current estimates and its application to high current MJR wires," *Adv. Cryo. Eng.*, vol. 44, pp. 919-925, 1998.

[8] E. J. Kramer, "Scaling laws for flux pinning in hard superconductors," *J. Appl. Phys.*, vol. 44 (3), pp. 1360-1370, 1973.

[9] M. Suenaga and R. L. Sabatini, "Effects of temperature ramp rate during heat treatment on hysteresis loss and critical current density of internal tin processed wires," *Proc. 9th US-Japan Workshop on High Field Materials, Wires and Conductors*, Kyoto, Japan, pp. 111-114, 1995.

[10] M. T. Naus, unpublished data.

[11] M. Onishi and H. Fujibuchi, "Reaction-diffusion in the Cu–Sn system," *Trans. Jpn. Inst. Met.*, vol. 16, pp. 539-547, 1975.

[12] J. D. Verhoeven, A. Efron, E. D. Gibson and C. C. Cheng, "Void formation in Nb_3Sn-Cu superconducting wire produced by the external tin process," *J. Appl. Phys.*, vol. 59 (6), pp. 2105-2113, 1986.